Mon. Not. R. Astron. Soc. **325,** 607–616 (2001)

The ages and colours of cool helium-core white dwarf stars

A. M. Serenelli,[1★†] L. G. Althaus,[1★‡] R. D. Rohrmann[2★†] and O. G. Benvenuto[1★§]
[1]*Facultad de Ciencias Astronómicas y Geofísicas, Universidad Nacional de La Plata, Paseo del Bosque S/N, (1900) La Plata, Argentina*
[2]*Observatorio Astronómico, Universidad Nacional de Córdoba, Laprida 854, (5000) Córdoba, Argentina*

Accepted 2001 February 19. Received 2001 February 16; in original form 2000 December 29

ABSTRACT

The purpose of this work is to explore the evolution of helium-core white dwarf stars in a self-consistent way with the predictions of detailed non-grey model atmospheres and element diffusion. To this end, we consider helium-core white dwarf models with stellar masses of 0.406, 0.360, 0.327, 0.292, 0.242, 0.196 and 0.169 $M_\odot$ and follow their evolution from the end of mass-loss episodes, during their pre-white dwarf evolution, down to very low surface luminosities.

We find that when the effective temperature decreases below 4000 K, the emergent spectrum of these stars becomes bluer within time-scales of astrophysical interest. In particular, we analyse the evolution of our models in the colour–colour and in the colour–magnitude diagrams and find that helium-core white dwarfs with masses ranging from ~0.18 to 0.3 $M_\odot$ can reach the turn-off in their colours and become blue again within cooling times much less than 15 Gyr and then remain brighter than $M_V \approx 16.5$. In view of these results, many low-mass helium white dwarfs could have had enough time to evolve to the domain of collision-induced absorption from molecular hydrogen, showing blue colours.

Key words: stars: atmospheres – stars: evolution – stars: fundamental parameters – stars: interiors – white dwarfs.

1 INTRODUCTION

The theoretical and observational study of white dwarf (WD) stars with helium cores (hereafter He WD) is a subject that has received increased attention particularly during the last few years. It is well known, for instance, that close binary evolution and mass-loss episodes are required to form low-mass He WDs within the age of the Galaxy (see Iben & Livio 1993 for a review). These He WDs populate the tail of low mass ($M < 0.4\,M_\odot$) in the WD mass distribution (Bergeron, Saffer & Liebert 1992; Bragaglia, Renzini & Bergeron 1995; Saffer, Livio & Yungelson 1998). The binary nature of these objects was first placed on a firm observational basis by Marsh (1995) and Marsh, Dhillon & Duck (1995). Since then, He WDs have been detected in numerous binary configurations involving either another WD or a neutron star (see, e.g., Lundgren et al. 1996; Moran, Marsh & Bragaglia 1997; Orosz et al. 1999; Maxted et al. 2000). Several He WDs have also been found in open clusters and in globular clusters (Landsman et al. 1997; Cool et al. 1998; Edmonds et al. 1999). Evolutionary models appropriate for the study of He WDs have recently been presented by Althaus & Benvenuto (1997), Benvenuto & Althaus (1998), Driebe et al. (1998) and Hansen & Phinney (1998a).

The determination of ages for the low-mass He WDs is a longstanding problem in the study of the evolution of these stars. As a matter of fact, cooling ages for He WDs are intimately related to the mass of the hydrogen envelope left before entering the final cooling track. Early investigations carried out by Webbink (1975) indicated that, as a result of massive hydrogen envelopes, hydrogen burning via the pp cycle remains the most important source of energy over most of the computed evolution, thus implying very long evolutionary time-scales. In agreement with this prediction, Alberts et al. (1996) and Sarna, Antipova & Ergma (1999) found that, on the basis of a detailed treatment of the binary evolution leading to the formation of these objects, the hydrogen-rich envelope surviving flash episodes is massive enough for residual hydrogen burning to be dominant even at low luminosities, thus resulting in very long cooling times. Massive hydrogen envelopes for He WDs have also been found by Driebe et al. (1998), who

★E-mail: serenell@fcaglp.fcaglp.unlp.edu.ar (AMS); althaus@fcaglp.fcaglp.unlp.edu.ar (LGA); rohr@oac.uncor.edu (RDR); obenvenuto@fcaglp.fcaglp.unlp.edu.ar (OGB)

†Fellow of the Consejo Nacional de Investigaciones Científicas y Técnicas (CONICET), Argentina.

‡Member of the Carrera del Investigador Científico y Tecnológico, Consejo Nacional de Investigaciones Científicas y Técnicas (CONICET), Argentina.

§Member of the Carrera del Investigador Científico, Comisión de Investigaciones Científicas de la Provincia de Buenos Aires, Argentina.

© 2001 RAS

have simulated the binary evolution by forcing a 1-$M_\odot$ model at the red giant branch to have a large mass-loss rate. Obviously, very large cooling ages, as derived from these evolutionary models, constrain the existence of He WDs with very low effective temperature ($T_{\rm eff}$) values. For example, the Driebe et al. (1998) model of 0.195 $M_\odot$ requires about 17 Gyr to evolve down to $T_{\rm eff} = 5000$ K, which exceeds any age range of interest. The possibility that the hydrogen envelope is considerably reduced by additional mass-loss episodes was considered by Iben & Tutukov (1986). These authors found that the last flash episode undergone by their 0.3-$M_\odot$ He WD model is strong enough to force the model to reach giant dimensions again, causing Roche lobe overflow. They found that the resulting mass transfer reduces the hydrogen envelope to such an extent that it is unable to support any further nuclear burning, thereby implying short cooling ages in the late stages of evolution. Finally, Benvenuto & Althaus (1998) and Hansen & Phinney (1998a) presented a detailed grid of He WD models based on the assumption that He WDs are formed with a relatively thin hydrogen envelope and thus hydrogen burning does not appreciably contribute to the luminosity budget of the star.

In the context of the foregoing discussion, binary systems composed of a millisecond pulsar and a low-mass He WD are particularly interesting, as they may place tight constraints on the evolution of He WDs. Indeed, the spin-down age of the pulsar provides an estimation of the age of the He WD companion, which can be compared with the predictions of evolutionary calculations for the WD. In this regard, the best-studied system belonging to this class is PSR J1012+5307, for which Lorimer et al. (1995) determined a spin-down age for the pulsar ($\tau_{\rm c}$) of 7 Gyr. In addition, atmospheric parameters of the He WD component have been derived by van Kerkwijk, Bergeron & Kulkarni (1996) and Callanan, Garnavich & Koester (1998) ($T_{\rm eff} \approx 8500$ K and $\log g \approx 6.3$–6.7). Evolutionary models of He WDs that predict thick hydrogen envelopes (Driebe et al. 1998) lead this low-mass WD ($M \approx 0.15$–$0.19\,M_\odot$) to an age which is consistent with the spin-down age of the pulsar. However, the large evolutionary time-scales predicted by these models are in disagreement with new observational data. In fact, a recent breakthrough has been the optical detection of the low-mass WD companion to the millisecond pulsar PSR B1855+09 by van Kerkwijk et al. (2000), who derived a $T_{\rm eff}$ value of 4800 ± 800 K for the WD companion. The mass of the WD in this binary system is accurately known – thanks to the Shapiro delay of the pulsar signal ($0.258^{+0.028}_{-0.016}\,M_\odot$; see Kaspi, Taylor & Ryba 1994). According to the models of Driebe et al. (1998), this low $T_{\rm eff}$ value corresponds to a WD cooling age of 10 Gyr, which is at odds with the characteristic age of the pulsar, $\tau_{\rm c} = 5$ Gyr. In addition, ages well above 10 Gyr are inferred from the models of Driebe et al. (1998) for the very cool WD companions to PSR J0034−0534 and PSR J1713+0747 (Hansen & Phinney 1998b). This may be an indication that such evolutionary models indeed overestimate the WD cooling ages, as discussed by van Kerkwijk et al. (2000). Finally, a recent population study of close double WDs in the Galaxy carried out by Yungelson et al. (2000) suggests that the low-mass He WDs have to cool much faster than suggested by the evolutionary models of Driebe et al. (1998).

Very recently, Althaus, Serenelli & Benvenuto (2001a,b) have presented new evolutionary calculations for He WDs aimed at exploring the role played by element diffusion in the occurrence of hydrogen shell flashes and, more importantly, to assess whether or not the mass of the hydrogen envelope can be considerably reduced by enhanced hydrogen burning during diffusion-induced, flash episodes. In particular, He WD models in the mass range 0.17–0.41 $M_\odot$ were evolved down to very low surface luminosities, starting from physically sound initial models generated by removing mass from a 1-$M_\odot$ model at appropriate stages of its red giant branch evolution. Most importantly, gravitational settling, chemical and thermal diffusion have been considered in these new calculations, and model evolution was computed in a self-consistent way with the evolution of element abundances as predicted by diffusion processes. Althaus et al. (2001a) found that element diffusion strongly affects the structure and evolution of He WDs, giving rise to a different cooling history depending on the stellar mass of the models. In particular, diffusion induces the occurrence of hydrogen shell flashes in He WDs with masses ranging from $\approx$0.18 to 0.41 $M_\odot$, which is in sharp contrast to the situation when diffusion is neglected. With respect to further evolution, these diffusion-induced flashes lead to hydrogen envelopes, thin enough so as to prevent stable nuclear burning from being an important energy source at advanced cooling stages.[1] This implies much shorter cooling ages when compared with the case in which diffusion is neglected (Driebe et al. 1998). In contrast, for masses lower than 0.18 $M_\odot$ (as is the case for the WD companion to PSR J1012+5307), nuclear burning is dominant even in the presence of diffusion, and cooling ages resemble those derived from models without diffusion.

The evolutionary calculations mentioned in the preceding paragraph have important implications when an attempt is made to compare the theoretical predictions on the WD evolution with expectations from millisecond pulsars, such as those mentioned earlier. As a matter of fact, these evolutionary models predict that as a result of element diffusion, evolution is accelerated to such an extent that the age discrepancy between the components of PSR B1855+09 vanishes completely. More specifically, these models lead to an age of 4 ± 2 Gyr for the WD component, in good agreement with the spin-down age of the pulsar. As mentioned, there also exist other millisecond pulsars with WD companions for which cooling and spin-down ages appear to be discrepant when the WD age is assessed from evolutionary models in which diffusion is not considered. This is the case for systems involving PSR J0034−053 and J1713+0747 (Hansen & Phinney 1998b), which most likely have very cool He WD companions. In contrast, evolutionary calculations including element diffusion result in ages in good agreement with the ages of such pulsars (Althaus et al. 2001a). Thus, age discrepancies between the predictions of standard evolutionary models and recent observational data of millisecond pulsar systems appear to be the result of element diffusion being ignored in such evolutionary calculations.

According to the evolutionary calculations of Althaus et al. (2001a), He WDs with stellar masses greater than $\approx$0.18 $M_\odot$ could reach very low $T_{\rm eff}$ stages well within the age of the Universe. In this connection, the WD LSH 3250 is particularly noteworthy – a surface luminosity of $\log(L/L_\odot) = -4.57 \pm 0.04$ (Harris et al. 1999) places it amongst the lowest luminosities known for any WD. It is highly likely that this WD is characterized by a helium core and a very low $T_{\rm eff}$ value (Harris et al. 1999) such that its emergent spectrum would be dominated by collision-induced absorption (CIA) from molecular hydrogen. Such a strong

[1] As Althaus et al. (2001a,b) did not invoke additional mass transfer when models return to the red giant region as a result of thermonuclear flashes, the surviving hydrogen envelope masses after flash episodes are upper limits.

molecular absorption causes cool WDs to become bluer as they age (Hansen 1998; Saumon & Jacobson 1999; Rohrmann 2001; see also Saumon et al. 1994 in the context of low-mass stars). WD evolutionary sequences based on detailed radiative-transfer calculations appropriate for very old carbon–oxygen WDs have recently been presented by Hansen (1998, 1999) and Salaris et al. (2000).

If cool low-mass He WDs are actually characterized by short cooling ages, as claimed by Althaus et al. (2001a) then many of them could present blue colours as a result of strong CIA from molecular hydrogen. With respect to these concerns, we realize it would be worthwhile to re-examine the ages of cool He WDs and at the same time to provide colours and magnitudes for these stars in a self-consistent way with the predictions of stellar evolution and element diffusion. This is the main aim of the present work, and to our knowledge such a type of calculation has never been performed. The present calculations are an improvement of those presented in Althaus et al. (2001a) with regard to the fact that here appropriate outer boundary conditions for the cooling models are derived on the basis of detailed non-grey model atmospheres (Rohrmann 2001). As far as cool WD ages are concerned, this is a very important point because WD cooling is very sensitive to the treatment of the outer boundary conditions. Another motivation for the present work is the determination of a theoretical luminosity function for He WDs from our new cooling curves. Details about our evolutionary code, initial models and diffusion treatment are briefly described in Section 2. In that section, we also detail the main characteristic of our model atmospheres. Results are presented in Section 3; in particular the evolution of our models in colour–magnitude diagrams (CMDs) is analysed. Finally, Section 4 is devoted to making some concluding remarks.

2 COMPUTATIONAL DETAILS

As stated in the introduction, one of the aims of this work is to provide a grid of ages, colours and magnitudes for WD cooling models appropriate for the study of old He WDs. This set of models covers a wide range of stellar masses as expected for such objects. In particular, the evolution of models with stellar masses of 0.406, 0.360, 0.327, 0.292, 0.242, 0.196 and 0.169 $M_{\odot}$ has been followed from the end of mass-loss episodes during the pre-WD evolution down to very low surface luminosities. WD evolution is computed in a self-consistent way with expectations from element diffusion, as done in Althaus et al. (2001a,b). This is in contrast to the grey-atmosphere approximation assumed in that work – here we consider a detailed treatment of the atmosphere which enables us to obtain accurate outer boundary conditions for our cooling models and colour indices as well.

Attention is focused mainly on the low-$T_{\rm eff}$ regime, where WD evolution is markedly dependent on the treatment of the extreme outer layers. When models reach such stages of evolution, element diffusion causes the bulk of hydrogen to float and helium and heavier elements to sink from outer layers (see Althaus et al. 2001a for details). This implies almost pure hydrogen atmospheres and justifies our use of atmosphere models for zero metallicity (see below).

In what follows, we briefly comment on the initial models, our atmospheric treatment and the input physics included in our evolutionary code.

2.1 Initial models

Reliable initial models have been obtained by simply removing mass from a 1-$M_{\odot}$ model at appropriate stages of the red giant branch evolution (see also Iben & Tutukov 1986 and Driebe et al. 1998). In this way, we were able to generate initial He WD models with stellar masses of 0.406, 0.360, 0.327, 0.292, 0.242, 0.196 and 0.169 $M_{\odot}$. It is worth mentioning that the resulting envelopes and hydrogen surface abundance of these initial models are in good agreement with those quoted by Driebe et al. (1998). We follow the further evolution of such initial configurations consistently with the predictions of element diffusion. As the stars enter the cooling branch, diffusion processes begin to play an important role. First, they cause hydrogen to float and other elements to sink, giving rise to outer layers of pure hydrogen. Simultaneously, chemical diffusion causes some hydrogen to move inwards to hotter layers, favouring the occurrence of a thermonuclear flash. Shortly after the flash begins, the star suddenly increases its radius and develops an outer convection zone which gets deep enough and reaches the helium-rich layers, thus modifying the composition of the outer layers. Over a time-scale of the order of a few hundred years the star evolves back to the red giant region and then finally to the cooling branch. At this stage, the evolutionary time-scale gets longer and diffusion begins to be important again, with the result that the outer layers are made up of hydrogen only. This in sharp contrast with the case in which diffusion is neglected. In that case, apart from convection, no other physical agent is able to drive hydrogen to the surface and therefore the chemical composition of the outer layer is fixed by the last episode of convective mixing (made up of hydrogen and helium in comparable proportions). Should the hydrogen envelope left after the flash episode be thick enough, another thermonuclear flash will be triggered by chemical diffusion. This sequence of events will be completed once the remaining hydrogen envelope is thin enough for hydrogen burning to become negligible. Thus the amount of hydrogen remaining after hydrogen flashes have ceased is markedly lower when diffusion is allowed to operate. This will produce not only a different cooling history, as mentioned in Section 1, but also noticeable changes in the structure of the star. In this regard, very different surface gravities result if diffusion is considered. For models with $M_{*} < 0.18\,M_{\odot}$ for instance, the surface gravity is reduced by almost 80 per cent as a result of element diffusion (see Althaus et al. 2001a for details).

After flash episodes have ceased and when the models have reached the final cooling branch, we compute the subsequent evolution by considering a detailed treatment of the atmosphere (see below). Here, evolution becomes slow enough for the purity of the outer layers to be established by diffusion processes.[2]

2.2 Model atmosphere

For a proper treatment of the cooling behaviour of He WDs, we have calculated the evolution of our He WD models in a self-consistent way with the predictions of detailed non-grey model atmospheres, which are described at length in Rohrmann (2001). Recently, the atmospheric code described in Rohrmann (2001) has been adapted for treating mixtures of hydrogen and helium. Here

[2] However, we should note that, as a result of the long diffusion time-scales at the base of the outer convection zone, metals accreted from the interstellar medium could be maintained in the outer layers of very cool He WDs for a long time (see Althaus & Benvenuto 2000).

we restrict ourselves to a few brief comments and refer the reader to that work for details and comparisons of such models with other relevant atmospheric calculations in the literature.

To begin with, our non-grey model atmospheres are constructed under the assumption of constant gravity, local thermodynamic equilibrium and plane-parallel geometry and include the hydrogen and helium species (zero metallicity). Energy transfer by radiation and convection are taken into account and the resulting equations are solved by means of a standard linearization technique. More specifically, the equation of radiative transfer (formulated in terms of the variable Eddington factors, see Auer & Mihalas 1970) and constant flux condition (radiative and convective contributions) are solved by means of an iterative procedure over linearized equations for a set of optical depth points and a frequency mesh. In the interest of minimizing computing time, we consider a partial linearization procedure in terms of temperature alone (Gustafsson 1971; Gustafsson & Nissen 1972). Only the Planck function and the convective flux are linearized while temperature corrections at each depth point are obtained by means of the Rybicki procedure, in which the resulting system of linear equations are ordered not in depth blocks but in frequency blocks (see Gustaffson & Nissen 1972).

Constitutive physics of our model atmospheres is based on an ideal equation of state.[3] The following species have been considered: H, H_2, e^-, H^-, H^+, H_2^+, H_3^+, He, He^+ and He^{++}. Although the abundances of species such as H_2^+ and H_3^+ are usually negligible, their presence affects the absorption and emission of radiation significantly (see Saumon et al. 1994). Partition functions for H and H_2; H_2^+ and H_3^+ are from Irwin (1981), Sauval & Tatum (1984) and Neale & Tennyson (1995), respectively. All relevant bound–free, free–free and scattering processes contributing to opacity have been included in our calculations. At low $T_{\rm eff}$ values, CIA by molecular hydrogen due to collisions with H_2 and He represents a major source of opacity in the infrared and dominates the shape of the emergent spectrum at low $T_{\rm eff}$. Here, we have included calculations for H_2–H_2 and H_2–He CIA cross-sections by Borysow, Jorgensen & Zheng (1997). Convection is treated within the formalism of the mixing length (ML2 version) and it has been included self-consistently in the equation of energy conservation and in the linearization procedure. It is worth mentioning that for $T_{\rm eff}$ values below 8000 K, the temperature profile becomes insensitive to the adopted parametrization of the mixing-length theory (Bergeron, Wesemael & Fontaine 1992). Broad-band colour indices have been calculated using the optical *BVRI* and infrared *JHK* passbands of Bessell & Brett (1988) and Bessell (1990), respectively, with calibration constants from Bergeron, Ruiz & Leggett (1997).

We note, as reported by Saumon et al. (1994) and Bergeron, Saumon & Wesemael (1995), that the numerical instabilities resulting from the competition between CIA by H_2 and H^- opacity develop in the $T_{\rm eff}$ regime from ≈3500–5000 K depending on the surface gravity. Such instabilities were overcome by the procedure suggested by these authors. Finally, the starting pressure and temperature values needed to integrate the envelope equations are given at an optical depth of $\tau \approx 25$. At this point the diffusion approximation for the radiative transfer can be assumed to be valid and the equations of stellar structure in the envelope, at the end of which we specify the outer boundary conditions to the evolutive models, can be integrated using Rosseland mean opacities.

[3] Non-ideal effects become important in hydrogen model atmospheres for $T_{\rm eff} < 2500$ K; see Saumon & Jacobson (1999).

2.3 Evolutionary code and diffusion treatment

The evolutionary calculations presented in this work were performed using the evolutionary code described in our previous work on WD evolution (see e.g. Althaus & Benvenuto 1997; Benvenuto & Althaus 1998; Althaus & Benvenuto 2000). In brief, our code includes a detailed and updated physical description, like for example OPAL radiative opacities (Iglesias & Rogers 1996) and molecular opacities (Alexander & Ferguson 1994); the equation of state for the low-density regime is an updated version of that of Magni & Mazzitelli (1979), whilst for the high-density regime we consider ionic contributions, Coulomb interactions, partially degenerate electrons, and electron exchange and Thomas–Fermi contributions at finite temperature. Conductive opacities and the various mechanisms of emission of neutrinos are taken from the formulation of Itoh and collaborators (see Althaus & Benvenuto 1997). Hydrogen burning is considered via a complete network of thermonuclear reaction rates corresponding to the proton–proton chain and the CNO bi-cycle. The chemical evolution resulting from element diffusion has also been considered. The diffusion calculations are based on the multi-component treatment of the gas developed by Burgers (1969), and gravitational settling, chemical and thermal diffusion have been taken into account. We mention that the WD evolution is calculated in a self-consistent way with the predictions of element diffusion. In addition, radiative opacities are calculated for metallicities as given by the varying abundances (more details are given in Althaus et al. 2001a and Althaus & Benvenuto 2000).

3 RESULTS

We begin by examining the evolutionary ages for some selected stellar masses. They are illustrated in Fig. 1 in which the $T_{\rm eff}$ versus

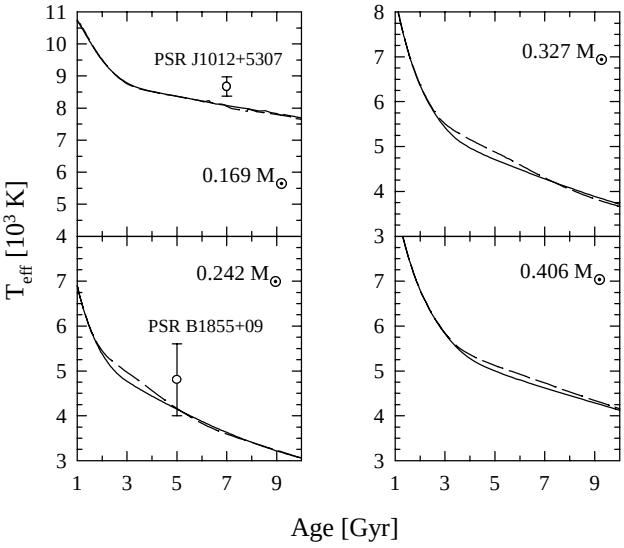

Figure 1. Effective temperature as a function of age for some selected values of the stellar mass. Solid lines correspond to the case when a detailed non-grey atmosphere is considered for deriving the outer boundary conditions for the WD evolution, and dashed lines to the situation when the standard grey approximation is used. Both sets of calculations take into account element diffusion. The observational data for the WD companion to the millisecond pulsars PSR B1855+09 and PSR J1012+5307 are included. Note that for more massive models and $4000 \lesssim T_{\rm eff} \lesssim 5500$ K, cooling ages become smaller in the case of a non-grey treatment for the atmosphere.

age relation is depicted together with the observational data for the WD companions to the millisecond pulsars PSR J1012+5307 and B1855+09 (Callanan et al. 1998 and van Kerkwijk et al. 2000, respectively). Only the evolution corresponding to the final cooling branch is depicted in the figure. For stellar masses greater than $\approx 0.18\,M_{\odot}$, models experience diffusion-induced hydrogen flashes and they are left with a small hydrogen mass and little nuclear burning, with the consequent result that cooling ages become substantially smaller when compared with the situation for less massive models, which do not suffer from flash episodes (see Althaus et al. 2001a). Note the good agreement with the observational predictions for both the pulsars. In particular, for the PSR B1855+09 companion, models with diffusion predict an age of 4 ± 2 Gyr in good agreement with the pulsar age. It is clear that element diffusion is an important ingredient in the evolution of He WDs that must be taken into account when an attempt is made to compare theoretical predictions with observational data.

Note that differences in the cooling of He WDs arise from the employment of detailed model atmospheres. Specifically, the inclusion of proper outer boundary conditions may decrease the cooling ages up to 1 Gyr in the range $4000 \lesssim T_{\rm eff} \lesssim 5500$ K. At such stages of evolution, the central temperature becomes strongly tied to the temperature stratification of the outer layers. In fact, when convection reaches the domain of degeneracy the central temperature drops substantially, and the star has initially an excess of internal energy to be radiated, thus giving rise to a lengthening of the evolutionary times during that epoch of evolution, as is borne out by the change of slope in the cooling curves shown in Fig. 1. At advanced stages of evolution, the thermal stratification of the envelope is affected by the use of non-grey atmospheres in such a way that the location of the maximum depth reached by the base of the outer convection zone is markedly shallower as compared with the prediction of the standard grey treatment for the atmosphere (see also Bergeron et al. 1997). This can be appreciated in Fig. 2 in which we show the evolution of the base of the outer convection zone in terms of $T_{\rm eff}$ for the 0.242-$M_{\odot}$ model. Clearly, when $T_{\rm eff}$ is decreased below 7000 K, the non-grey treatment predicts a shallower outer convection zone (this behaviour is essentially the same irrespective of the stellar mass of the model). As a result, convection reaches the degenerate core at lower $T_{\rm eff}$ values in such models, and accordingly the drop in the central temperature takes place later than that of the grey models, as shown in Fig. 3. This behaviour explains the trend of the cooling curves in both sets of calculations.

Another interesting issue of our evolutionary calculations, also related to the extent of the outer convection zone, is the following. As noted by Althaus et al. (2001a), the hydrogen envelope left after diffusion-induced flash episodes may be thin enough to enable convection to mix it with the underlying helium layers at advanced stages of evolution. In fact, these authors found that over a time interval of 2 Gyr, models with masses of $\approx 0.2\,M_{\odot}$ are characterized by outer layers made up of hydrogen and helium by the time they have cooled down to $T_{\rm eff} \approx 5000$ K. As mentioned (see Fig. 2), the use of detailed model atmospheres to derive outer boundary conditions for evolving WDs gives rise to shallower outer convection zones, as compared with the grey treatment considered in Althaus et al. (2001a). As a result, no mixing episodes occur at all and the envelope of our He WD models remains as pure hydrogen down to the end of the cooling sequence.

From the cooling curves, we can estimate the predicted number density of He WDs as a function of luminosity. To this end we have translated the cooling curves for our set of models into a total luminosity function according to the relation given by

$$\Phi = \sum_i n_i, \qquad (1)$$

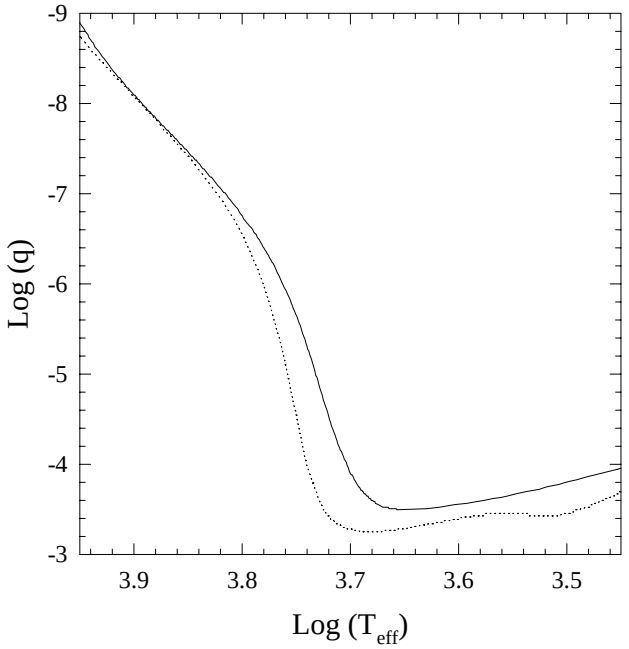

Figure 2. The location of the base of the outer convection zone in terms of the outer mass fraction q as a function of the effective temperature for 0.242-$M_{\odot}$ He WD models. Solid and dotted lines correspond, respectively, to the non-grey and grey treatment for the atmosphere. Note that the outer convection zone is shallower when the detailed treatment for the atmosphere is taken into account.

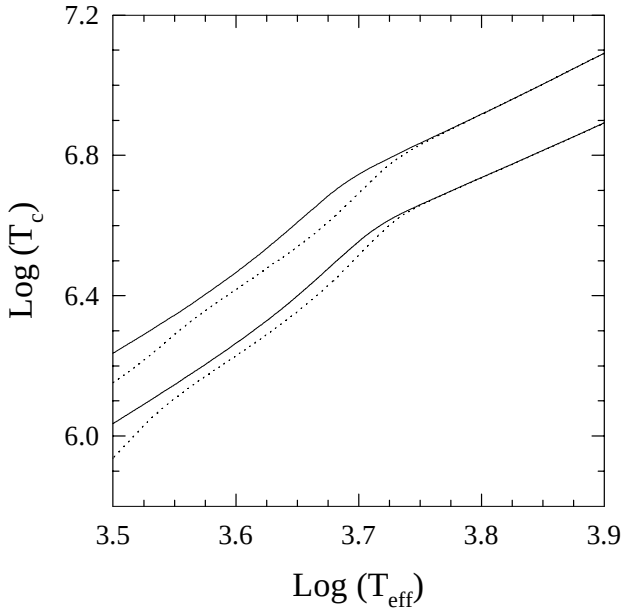

Figure 3. Central temperature as a function of effective temperature for 0.242- and 0.406-$M_{\odot}$ He WD models (upper and lower curves, respectively). For each stellar mass, solid and dotted lines correspond, respectively, to the non-grey and grey treatment for the atmosphere.

with

$$n_i = \frac{k_i \Delta t}{V}. \quad (2)$$

Here, k_i is the birthrate of He WDs of a given stellar mass, the summation of which is normalized to the birthrate at which He WDs are produced ($0.14\,\mathrm{yr}^{-1}$; see Iben, Tutukov & Yungelson 1997), n_i is the number density of the He WDs (single luminosity function) of a given mass in the magnitude interval $M_b - 0.5$ to $M_b + 0.5$, Δt is the time interval required by the model for it to evolve from magnitude $M_b - 0.5$ to $M_b + 0.5$ and V is the volume of the Galactic disc ($3 \times 10^{11}\,\mathrm{pc}^3$). On the basis of these assumptions, the resulting single luminosity functions for our models are displayed in Fig. 4. A striking feature shown in this figure is the spikes at intermediate luminosities, which correspond to the evolutionary phases prior to the onset of flash episodes where evolution slows down. At high luminosities, the theoretical distribution of each He WD exhibits a bump. These bumps are a consequence of the slow rate of evolution before the models enter their cooling branch. To understand the behaviour of n_i at high luminosities, it should be kept in mind that as a result of thermonuclear flashes, models reach the high surface luminosity phase more than once. Less massive models experience many flash episodes; thus their resulting luminosity functions show more extended bumps.

The total luminosity function, Φ, results from the superposition of the single number density of He WDs and it is illustrated by Fig. 5. Note that over most of the given surface luminosity range, the total luminosity function exhibits a rather monotonically increasing trend down to $\log(L/\mathrm{L}_\odot) \approx -2.5$. Little of the behaviour of the individual luminosity function remains. This is expected because flash episodes occur at different surface luminosities depending on the stellar mass with the result that the spikes cancel themselves out. At $\log(L/\mathrm{L}_\odot) \approx -2.5$, the luminosity function shows a local maximum as a result of the contribution of models that do not experience hydrogen-shell flashes. Indeed, as mentioned earlier, such models are characterized by stable nuclear burning even at low $T_{\rm eff}$ values, with the consequent result that their evolution is considerably slowed down. More specifically, at such a luminosity, the 0.169-$\mathrm{M}_\odot$ model is characterized by an age of $\approx$14 Gyr; so it is not expected to contribute to the number density of He WDs at lower luminosities within the age of the Universe. At $\log(L/\mathrm{L}_\odot) \approx -4$, the luminosity function shows a small bump. As explained earlier, when convection reaches the degenerate core, there is initially an excess of energy to get rid of and the cooling process is slowed down, thus leading to the small bump in the luminosity function at low values of stellar luminosities. Finally, we should note that we have considered single He WDs, that is we have neglected a possible merger of those He WDs formed in binary systems with small separation for gravitational wave radiation to lead to a merger of the components on time-scales shorter than the Hubble time. Accordingly, care should be taken when comparing our theoretical luminosity functions at low luminosities with the observations.

The evolution of the emergent flux distribution for the 0.292-$\mathrm{M}_\odot$ He WD model at some selected $T_{\rm eff}$ values can be seen in Fig. 6. The results of the non-grey atmosphere (solid lines) are compared with the blackbody predictions (dashed lines) at the same $T_{\rm eff}$ value. We want to stress again that by the time the models reach the $T_{\rm eff}$ range considered in Fig. 6, element diffusion has already

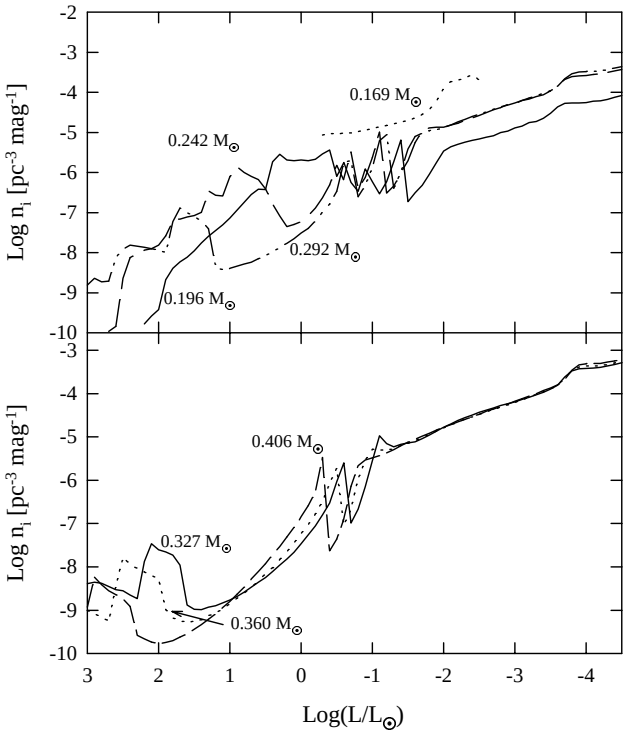

Figure 4. Single luminosity function versus surface luminosity for our He WD models. The spikes at intermediate luminosities correspond to the evolutionary phases before the onset of flash episodes and the bumps at high luminosities reflect the slow rate of evolution before the models enter their cooling branch. Less massive models (top panel) experience various flash episodes, so they reach the blue part of the HR diagram many times. Accordingly, the resulting luminosity functions show more extended bumps.

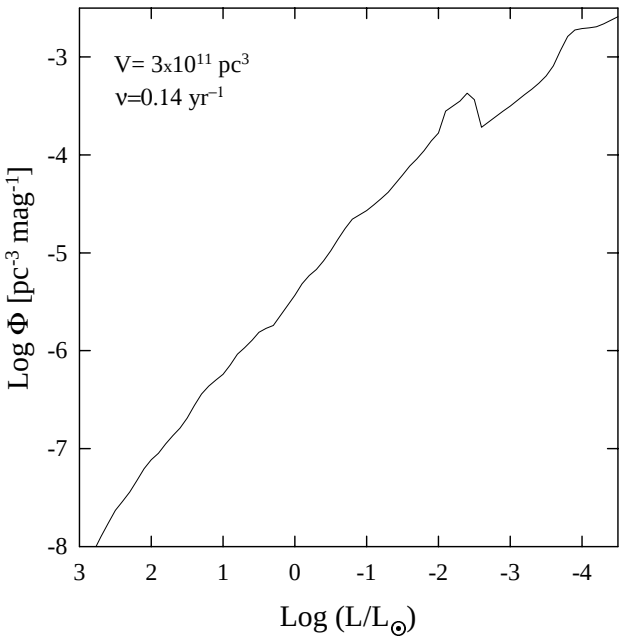

Figure 5. Total luminosity function (resulting from the superposition of the single number density of He WDs given in Fig. 4) versus surface luminosity for our He WD models. The bump at $\log(L/\mathrm{L}_\odot) \approx -2$ is due to the slow rate of evolution characterizing our lowest mass model, which cannot reach lower luminosities within a Hubble time. Such low-mass He WDs are thus not expected to contribute to the luminosity function at very low luminosities. For details, see text.

caused heavier elements than hydrogen to sink below the outer layers. So, our evolving He WD models at such advanced stages of evolution are characterized by pure hydrogen outer layers. At high temperatures, the H^- opacity is dominant. Since this opacity is almost independent of frequency, the emergent flux resembles that of the blackbody spectrum. The main observation we can make from this figure is that when $T_{\rm eff}$ is lowered below 4000 K, the emergent spectrum becomes bluer. This effect, reported also by Saumon et al. (1994) and more recently by Hansen (1998, 1999), Saumon & Jacobson (1999), Salaris et al. (2000) and Rohrmann (2001) (particularly in the context of carbon–oxygen WDs), is due to the strong CIA opacity by molecular hydrogen that reduces the infrared flux and forces radiation to emerge at larger frequencies. As a result, cool low-mass He WDs become bluer as they age. Needless to say, this effect also affects the colour–colour diagrams and colour–magnitude diagrams (CMDs). Indeed, most colour indices show a pronounced turn-off at low $T_{\rm eff}$ values and they become bluer after reaching a maximum. This is well illustrated by Fig. 7 in which the $(B-V, V-K)$ two-colour diagram is shown for all of our He WD models together with the observational data for DA and non-DA WDs according to Bergeron, Leggett & Ruiz (2001). The peculiar WD LHS 3250 analysed by Harris et al. (1999) is also included in the figure. Note also that for $T_{\rm eff}$ below 5000 K, colours become markedly bluer in this diagram.

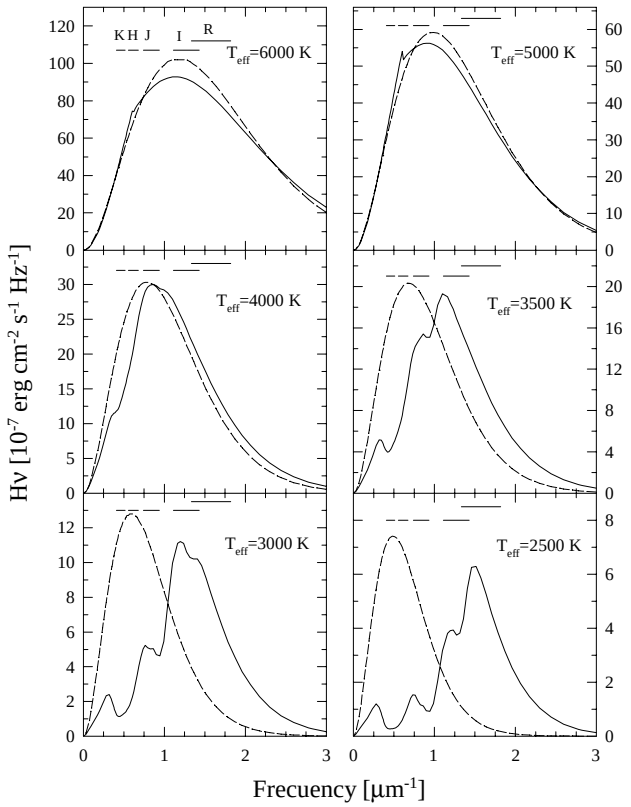

Figure 6. Emergent spectrum for the 0.292-$M_\odot$ He WD model at selected values of effective temperature (as indicated within each figure). Solid lines depict the results of the non-grey atmosphere, whilst dashed lines correspond to the blackbody predictions at the same temperature. Short solid lines indicate the location of the transmission functions for the filters K, H, J, I and R. Note that as effective temperature is lowered, the spectrum becomes bluer. This is a direct consequence of the CIA opacity which is dominant at low effective temperatures.

Now we analyse the evolution of our He WD models in the CMD. In particular, we show in Figs 8 and 9 the behaviour of the absolute visual magnitude M_V for our models as a function of the colour indices $V-I$ and $B-V$, respectively. The observational samples for cool DA (open circles) and non-DA (open triangles) WDs of Bergeron et al. (2001) are also included in the figure, as well as the location of the WD LHS 3250 according to Harris et al. (1999). For the 0.169-$M_\odot$ model, only the phase of low M_V values is depicted because such a model would require exceedingly high ages to evolve to lower luminosities. In contrast, more massive models can reach high magnitudes within a Hubble time. Indeed, as can be seen from the figure, He WD models in the mass range from $\sim$0.18 to 0.3 $M_\odot$ can reach the turn-off point and become blue again within cooling times less than 15 Gyr. Specifically, such models have cooling ages of 6–9 Gyr at the turn-off, which occurs at $M_V \approx 16$. Note that with further evolution, they remain brighter than $M_V \approx 16.5$. The results presented here raise the possibility that many low-mass He WDs could have had enough time to evolve beyond the turn-off point and could have presented blue colours. The cool WD LHS 3250 analysed by Harris et al. (1999) could be an example of such WDs. More massive He WDs present a similar trend in their colour–magnitude evolution but the ages involved are considerably larger. For instance, the 0.406-$M_\odot$ model needs about 13 Gyr to reach the turn-off in the $V-I$ colour index. We would like to stress again the fact that the short cooling ages characterizing such models are due to the role played by element diffusion during the evolutionary phases prior to those computed here. In fact, element diffusion leads to hydrogen shell flashes during which the mass of the hydrogen envelope is reduced to such an extent that nuclear burning becomes negligible on the final cooling track, thus implying much shorter cooling ages compared with the situation when diffusion is neglected (such as in Driebe et al.

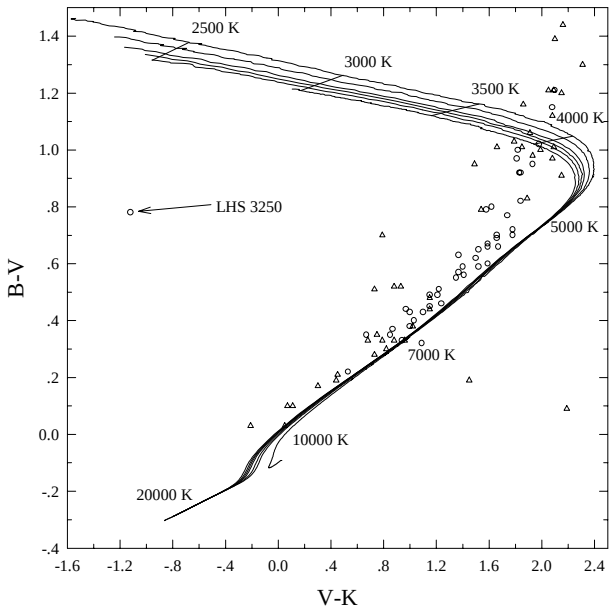

Figure 7. $(B-V, V-K)$ colour–colour diagram for our He WD models with masses of (from top to bottom) 0.196, 0.242, 0.292, 0.327, 0.360 and 0.406 $M_\odot$. Points of equal effective temperature are represented by thin lines and labelled with the corresponding values. The observational samples for cool DA (open circles) and non-DA (open triangles) WDs of Bergeron et al. (2001) are also included in the figure, as well as the location of the WD LHS 3250 according to Harris et al.'s (1999) determinations.

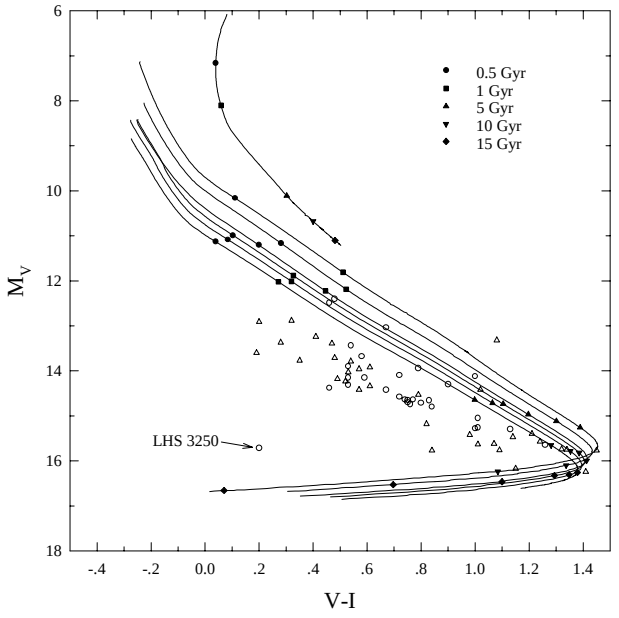

Figure 8. Absolute visual magnitude M_V in terms of the colour index $V - I$ for our He WD models with masses of (from top to bottom) 0.169, 0.196, 0.242, 0.292, 0.327, 0.360 and 0.406 $M_\odot$. On each curve, filled symbols indicate cooling ages, as explained within the figure. The observational samples for cool DA (open circles) and non-DA (open triangles) WDs of Bergeron et al. (2001) are also included in the figure, as well as the location of the WD LHS 3250 according to the observations of Harris et al. (1999). Models with $M \geq 0.196\,M_\odot$ exhibit a pronounced turn-off at advanced stages of evolution and then become bluer with further evolution. According to our evolutionary calculations, He WDs with masses from ~ 0.18 to $0.3\,M_\odot$ could evolve beyond the turn-off well within 15 Gyr.

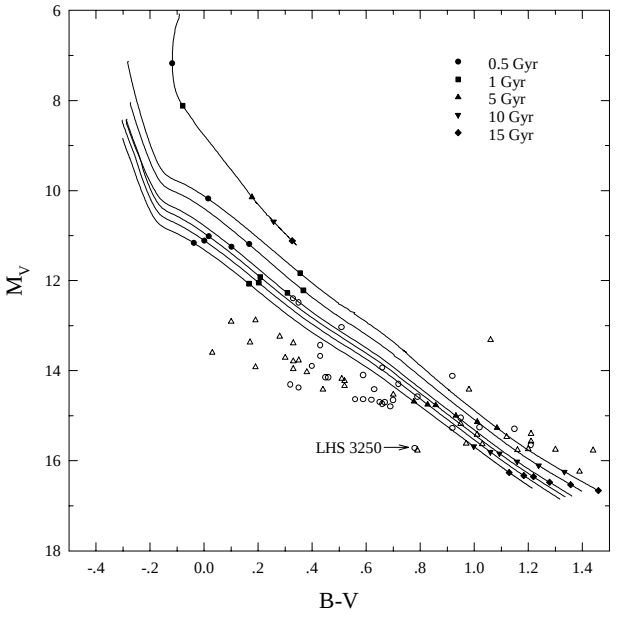

Figure 9. Same as Fig. 8 but for the colour index $B - V$. Unlike the $V - I$, the $B - V$ colour index does not show a turn-off at low effective temperatures.

1998). The CMD for the $B - V$ colour index is shown in Fig. 9. Note that the $B - V$ colour index does not show a turn-off at low $T_{\rm eff}$. We should mention that for $T_{\rm eff}$ values above $\approx$8000 K, our predictions of the $B - V$ show discrepancies compared with those of Bergeron et al. (1995) because in our calculations we have not considered the effects of line broadening opacities.

Finally, we list in Table 1 the colour indices for our 0.169-, 0.242-, 0.327- and 0.406-$M_\odot$ He WD models at some selected low $T_{\rm eff}$ values. In addition, for each stellar mass and $T_{\rm eff}$ value, we provide the surface gravity (g), the age (in Gyr), the absolute visual magnitude (M_V) and the bolometric correction (BC). The latter is calculated according to (see Bergeron, Wesemael & Beauchamp 1995)

$$BC = 2.5 \log \int_0^\infty H_\lambda S_\lambda^V \, {\rm d}\lambda - 10 \log T_{\rm eff} + 15.6165, \qquad (3)$$

where H_λ and S_λ^V are the monochromatic emergent flux at temperature $T_{\rm eff}$ and the transmission function of the V filter, respectively.

4 CONCLUSIONS

The present study is aimed at exploring the evolution of WD stars with helium cores (He WDs). The results are based on very detailed non-grey model atmospheres which allow us to derive accurate boundary conditions for the evolving models. Emphasis has been placed on the advanced stages of the evolution of these objects where WD evolution is markedly dependent on the treatment of the atmosphere. The evolutionary phases leading to the formation of cool He WDs have been explored in detail by Althaus et al. (2001a), who found that the inclusion of element diffusion in evolutionary calculations for He WDs leads to hydrogen envelopes thin enough for stable nuclear burning to play a minor role in the late stages of evolution. Here, we improved the above-mentioned calculations by following the evolution of He WD models in a self-consistent way with the predictions of non-grey model atmospheres. Another motivation for the present work was to construct a theoretical luminosity function for He WDs and to provide colour indices and magnitudes for these WDs self-consistently with stellar evolution and element diffusion.

In particular, we have considered He WD models with stellar masses of 0.406, 0.360, 0.327, 0.292, 0.242, 0.196 and 0.169 $M_\odot$, the evolution of which has been followed from the end of mass-loss episodes during the pre-WD evolution down to very low surface luminosities.

We find that when $T_{\rm eff}$ decreases below 4000 K, the emergent spectrum of the He WDs becomes bluer and not redder, as reported by other investigators. We also analyse the evolution of our He WD models in the CMDs and find that the He WDs with masses ranging from $\sim$0.18 to $0.3\,M_\odot$ can reach the turn-off in their colours and become blue again within cooling times much less than 15 Gyr and then remain brighter than $M_V \approx 16.5$. This is an interesting result because it raises the possibility that many low-mass He WDs could have had enough time to evolve beyond the turn-off point and present blue colours. Such short cooling times have also been derived by Althaus et al. (2001a,b) on the basis of detailed evolutionary models that consider the pre-WD evolution and the effects of element diffusion. As shown by these authors, these new models solve the discrepancy between the predictions of standard evolutionary calculations (which do not consider element diffusion, such as Driebe et al. 1998) for He WDs and the age of some millisecond pulsar companions. The detection of blue, low-mass He WDs at very low $T_{\rm eff}$ would place the theoretical predictions of our models on a firm observational basis.[4]

[4] Complete tables containing the results of the present calculations are available at http://www.fcaglp.unlp.edu.ar/~althaus/ or upon request to the authors at their e-mail addresses.

Table 1. Selected stages for 0.169-, 0.242-, 0.327- and 0.406-$M_\odot$ He WD models.

$M_*/M_\odot$	$T_{\rm eff}$	Log(g)	Age (Gyr)	$B-V$	$V-R$	$V-K$	$R-I$	$J-H$	$H-K$	BC	M_V
0.169	10000	6.0621	1.56	−0.01	0.04	0.03	0.06	0.02	−0.06	−0.34	8.70
"	9500	6.1624	1.99	0.04	0.07	0.15	0.08	0.04	−0.06	−0.29	9.11
"	9000	6.2555	2.60	0.10	0.11	0.30	0.11	0.07	−0.05	−0.25	9.55
"	8500	6.3499	4.11	0.16	0.14	0.46	0.14	0.10	−0.04	−0.23	10.01
"	8000	6.4256	7.63	0.22	0.18	0.64	0.18	0.14	−0.02	−0.21	10.44
"	7500	6.4796	11.45	0.28	0.22	0.82	0.22	0.18	−0.01	−0.19	10.84
"	7050	6.5265	16.52	0.34	0.25	1.00	0.25	0.21	0.00	−0.17	11.21
0.242	10000	6.9458	0.32	0.03	0.07	0.08	0.07	0.03	−0.06	−0.37	10.54
"	9500	6.9616	0.37	0.08	0.09	0.20	0.09	0.05	−0.05	−0.32	10.76
"	9000	6.9780	0.44	0.13	0.12	0.34	0.12	0.08	−0.04	−0.28	11.00
"	8500	6.9945	0.53	0.18	0.15	0.49	0.15	0.11	−0.03	−0.25	11.26
"	8000	7.0119	0.64	0.23	0.19	0.65	0.18	0.14	−0.02	−0.22	11.53
"	7500	7.0291	0.78	0.29	0.22	0.83	0.22	0.18	−0.01	−0.20	11.83
"	7000	7.0464	0.96	0.35	0.26	1.02	0.26	0.22	0.01	−0.18	12.15
"	6500	7.0637	1.19	0.43	0.30	1.23	0.30	0.26	0.03	−0.16	12.50
"	6000	7.0818	1.48	0.52	0.35	1.48	0.36	0.30	0.06	−0.17	12.90
"	5500	7.1044	1.88	0.64	0.42	1.76	0.42	0.34	0.09	−0.21	13.38
"	5000	7.1423	2.50	0.77	0.50	2.11	0.50	0.39	0.13	−0.31	13.99
"	4500	7.1779	3.80	0.91	0.59	2.36	0.59	0.38	0.09	−0.45	14.68
"	4000	7.1974	5.54	1.04	0.67	2.15	0.67	0.10	−0.01	−0.51	15.29
"	3500	7.2082	7.57	1.15	0.73	1.42	0.70	−0.18	−0.19	−0.37	15.76
"	3000	7.2149	10.38	1.25	0.74	0.39	0.56	−0.30	−0.32	−0.07	16.14
"	2500	7.2207	15.20	1.36	0.65	−0.79	0.00	−0.21	−0.48	0.34	16.54
0.327	10000	7.3138	0.57	0.05	0.07	0.10	0.07	0.03	−0.06	−0.38	11.15
"	9500	7.3240	0.68	0.09	0.10	0.22	0.09	0.05	−0.05	−0.34	11.35
"	9000	7.3339	0.80	0.14	0.13	0.36	0.12	0.08	−0.04	−0.30	11.57
"	8500	7.3433	0.94	0.19	0.16	0.50	0.15	0.11	−0.03	−0.26	11.81
"	8000	7.3524	1.12	0.24	0.19	0.66	0.18	0.14	−0.02	−0.23	12.07
"	7500	7.3613	1.33	0.29	0.22	0.83	0.22	0.18	−0.01	−0.20	12.34
"	7000	7.3702	1.58	0.36	0.26	1.02	0.26	0.22	0.01	−0.18	12.63
"	6500	7.3794	1.90	0.43	0.30	1.23	0.30	0.26	0.03	−0.16	12.96
"	6000	7.3899	2.31	0.53	0.36	1.47	0.36	0.29	0.06	−0.16	13.34
"	5500	7.4041	2.89	0.65	0.42	1.76	0.43	0.33	0.10	−0.21	13.80
"	5000	7.4258	3.91	0.77	0.50	2.10	0.50	0.39	0.12	−0.31	14.37
"	4500	7.4451	5.95	0.91	0.59	2.30	0.59	0.35	0.07	−0.44	15.00
"	4000	7.4559	8.41	1.03	0.67	2.02	0.66	0.04	−0.03	−0.47	15.57
"	3500	7.4622	11.39	1.13	0.72	1.27	0.68	−0.21	−0.20	−0.32	16.02
"	3000	7.4665	15.67	1.23	0.72	0.26	0.51	−0.30	−0.32	−0.01	16.39
"	2500	7.4701	23.95	1.33	0.61	−0.96	−0.10	−0.20	−0.51	0.39	16.79
0.406	10000	7.5664	0.71	0.06	0.08	0.12	0.07	0.03	−0.06	−0.39	11.55
"	9500	7.5722	0.82	0.10	0.11	0.24	0.10	0.05	−0.05	−0.35	11.75
"	9000	7.5783	0.95	0.14	0.13	0.37	0.12	0.08	−0.04	−0.31	11.96
"	8500	7.5838	1.11	0.19	0.16	0.51	0.15	0.11	−0.03	−0.27	12.18
"	8000	7.5897	1.30	0.24	0.19	0.67	0.18	0.14	−0.02	−0.24	12.43
"	7500	7.5952	1.55	0.29	0.22	0.84	0.22	0.18	−0.01	−0.21	12.69
"	7000	7.6010	1.85	0.36	0.26	1.02	0.26	0.22	0.01	−0.18	12.98
"	6500	7.6072	2.25	0.44	0.30	1.23	0.30	0.25	0.03	−0.16	13.29
"	6000	7.6139	2.77	0.53	0.36	1.47	0.36	0.29	0.06	−0.16	13.66
"	5500	7.6238	3.52	0.65	0.42	1.75	0.42	0.33	0.10	−0.21	14.11
"	5000	7.6374	5.00	0.77	0.50	2.09	0.50	0.38	0.12	−0.31	14.66
"	4500	7.6482	7.71	0.91	0.59	2.25	0.59	0.33	0.06	−0.43	15.27
"	4000	7.6543	10.83	1.02	0.66	1.92	0.66	0.01	−0.06	−0.44	15.80
"	3500	7.6580	14.68	1.12	0.71	1.15	0.67	−0.22	−0.22	−0.28	16.23
"	3000	7.6607	20.37	1.21	0.71	0.16	0.47	−0.30	−0.33	0.02	16.60

ACKNOWLEDGMENTS

We thank our anonymous referee whose comments and suggestions greatly improved the original version of this paper.

REFERENCES

Alberts F., Savonije G. J., van den Heuvel E. P. J., Pols O. R., 1996, Nat, 380, 676

Alexander D. R., Ferguson J. W., 1994, ApJ, 437, 879

Althaus L. G., Benvenuto O. G., 1997, ApJ, 477, 313

Althaus L. G., Benvenuto O. G., 2000, MNRAS, 317, 952

Althaus L. G., Serenelli A. M., Benvenuto O. G., 2001a, MNRAS, 471

Althaus L. G., Serenelli A. M., Benvenuto O. G., 2001b, ApJ, in press

Auer L. H., Mihalas D., 1970, MNRAS, 149, 65

Benvenuto O. G., Althaus L. G., 1998, MNRAS, 293, 177

Bergeron P., Leggett S. K., Ruiz M. T., 2001, ApJS, 133, 413

Bergeron P., Ruiz M. T., Leggett S. K., 1997, ApJS, 108, 339

Bergeron P., Saffer R. A., Liebert J., 1992, ApJ, 394, 228
Bergeron P., Saumon D., Wesemael F., 1995, ApJ, 443, 764
Bergeron P., Wesemael F., Beauchamp A., 1995, PASP, 107, 1047
Bergeron P., Wesemael F., Fontaine G., 1992, ApJ, 387, 288
Bessell M. S., 1990, PASP, 102, 1181
Bessell M. S., Brett J. M., 1988, PASP, 100, 1134
Borysow A., Jorgensen U. G., Zheng C., 1997, A&A, 324, 185
Bragaglia A., Renzini A., Bergeron P., 1995, ApJ, 443, 735
Burgers J. M., 1969, Flow Equations for Composite Gases. Academic, New York
Callanan P. J., Garnavich P. M., Koester D., 1998, MNRAS, 298, 211
Cool A. M., Grindlay J. E., Cohn H. N., Lugger P. M., Bailyn C. D., 1998, ApJ, 508, L75
Driebe T., Schönberner D., Blöcker T., Herwig F., 1998, A&A, 339, 123
Edmonds P. D., Grindlay J. E., Cool A. M., Cohn H. N., Lugger P. M., Bailyn C. D., 1999, ApJ, 516, 250
Gustaffson B., 1971, A&A, 10, 187
Gustaffson B., Nissen P. E., 1972, A&A, 19, 261
Hansen B. M. S., 1998, Nat, 394, 860
Hansen B. M. S., 1999, ApJ, 520, 680
Hansen B. M. S., Phinney E. S., 1998a, MNRAS, 294, 557
Hansen B. M. S., Phinney E. S., 1998b, MNRAS, 294, 569
Harris H. C., Dahn C. C., Vrba F. J., Henden A. A., Liebert J., Schmidt G. D., Reid I. N., 1999, ApJ, 524, 1000
Iben I., Jr, Livio M., 1993, PASP, 105, 1373
Iben I., Jr, Tutukov A. V., 1986, ApJ, 311, 742
Iben I., Jr, Tutukov A. V., Yungelson L., 1997, ApJ, 475, 291
Iglesias C. A., Rogers F. J., 1996, ApJ, 464, 943
Irwin A. W., 1981, ApJS, 45, 261
Kaspi V. M., Taylor J. H., Ryba M. F., 1994, ApJ, 428, 713
Landsman W., Aparicio J., Bergeron P., Di Stefano R., Stecher T. P., 1997, ApJ, 481, L93
Lorimer D. R., Festin L., Lyne A. G., Nicastro L., 1995, Nat, 376, 393
Lundgren S. C., Cordes J. M., Foster R. S., Wolszczan A., Camilo F., 1996, ApJ, 458, L33
Magni G., Mazzitelli I., 1979, A&A, 72, 134
Marsh T. R., 1995, MNRAS, 275, L1
Marsh T. R., Dhillon V. S., Duck S. R., 1995, MNRAS, 275, 828
Maxted P. F. L., Marsh T. R., Moran C. H. J., Zan Z., 2000, MNRAS, 314, 334
Moran C., Marsh T. R., Bragaglia A., 1997, MNRAS, 288, 538
Neale L., Tennyson J., 1995, ApJ, 454, L169
Orosz J. A., Wade R. A., Harlow J. J. B., Thorstensen J. R., Taylor C. J., Eracleous M., 1999, AJ, 117, 1598
Rohrmann R. D., 2001, MNRAS, 323, 699
Saffer R. A., Livio M., Yungelson L. R., 1998, ApJ, 504, 392
Salaris M., García-Berro E., Hernanz M., Isern J., Saumon D., 2000, ApJ, in press
Sarna M. J., Antipova J., Ergma E., 1999, in Solheim J.-E., Meistas E. G., eds, 11th ASP Conf. Ser., Vol. 169, European Workshop on White Dwarfs. Astron. Soc. Pac., San Francisco, p. 400
Saumon D., Jacobson S. B., 1999, ApJ, 511, L107
Saumon D., Bergeron P., Lunine J. I., Hubbard W. B., Burrows A., 1994, ApJ, 424, 333
Sauval A. J., Tatum J. B., 1984, ApJS, 56, 193
van Kerkwijk M. H., Bergeron P., Kulkarni S. R., 1996, ApJ, 467, L89
van Kerkwijk M. H., Bell J. F., Kaspi V. M., Kulkarni S. R., 2000, ApJ, 530, L37
Yungelson L. R., Nelemans G., Portegies Zwart S. F., Verbunt F., 2000, in Vanbeveren D., ed., The influence of binaries in stellar populations, in press (astro-ph/0011248)
Webbink R. F., 1975, MNRAS, 171, 555

This paper has been typeset from a TEX/LATEX file prepared by the author.